Investigation on the Phase Noise and EVM of Digitally Modulated Millimeter Wave Signal in WDM Optical Heterodyning System

Tong Shao, Flora Paresys, Ghislaine Maury, Yannis Le Guennec, Beatrice Cabon

Investigation on the Phase Noise and EVM of Digitally Modulated Millimeter Wave Signal in WDM Optical Heterodyning System

Tong Shao, Flora Parésys, Ghislaine Maury, Yannis Le Guennec, and Béatrice Cabon

***Abstract*—In this paper, theoretical model on phase noise in self-heterodyning optical system for mmW generation is proposed. Phase noise is impacted by optical path difference between both optical tones and laser source coherence time, but also by RF generators phase noise. Phase noise measurements of the mmW signal and RF sources have been realized to discuss the validity of the model. Based both on the theoretical approach and on the phase noise characterizations, an error vector magnitude (EVM) model is developed to quantify the impact of the optical self-heterodyning output phase noise on up-converted broadband digital signal (ECMA 387 standard). .**

***Index Terms*—radio over fiber (RoF), optical heterodyning, wavelength division multiplexing (WDM), phase noise, optical delay, error vector magnitude (EVM).**

I. Introduction

BROADBAND millimeter wave (mmW) transmission has attracted great interest because it meets the demand of high-speed data (>1 gigabit per second) wireless transmission. Nevertheless, due to the short transmission range of mmW signal transmission, many base stations (BSs) are required in the network infrastructure and to achieve high data rate mmW communications, low phase noise mmW local oscillators (LO) should be used in each BS [1], which may increase the overall system cost.

Radio-over-fiber (RoF) technology has raised great interest in the last decade for optical generation and transmission of RF signals [2]. In particular, broadband mmW generation by optical heterodyning has been intensively investigated in order to centralize mmW generation and to simplify the design of mmW BSs. Optical heterodyning by two independent lasers requires complex optical phase locking between two lasers to realize low phase noise mmW generation [3] [4]. Coherent heterodyning (or self-heterodyning) is a common technique to generate low phase noise mmW by beating of two coherent optical tones [5-9]. One solution for self-heterodyning is to use mode locked laser diodes (MLLD) exhibiting multi wavelength output [5-7]. Another solution is to use a single longitudinal mode laser, such as commercial DFB laser, coupled with external modulation technique to generate a double sideband suppressed carrier (DSB-SC) light wave [8, 9]. The above cited techniques can be easily scaled to a multi-user scheme: each BS is addressed with the 2 dedicated optical tones to generate the mmW signal by using optical filtering. Commercial WDM demultiplexers (DEMUX) can be used for this purpose, as in [4], where experiments have been conducted using super continuum (SC) light source, with a frequency interval between the optical spectral lines of 25 GHz. The WDM device has been employed to select two optical subcarriers with 50 GHz frequency interval to address the dedicated BS. Phase noise measurements have shown that optical self-heterodyning could provide low noise mmW [5].

Nevertheless, a particular attention has to be paid to optical self-heterodyning system design because of the coherent nature of this experiment scheme in [4-7] due to the different optical paths between optical filter and coupler [10]. Indeed, the difference between the paths carrying the 2 beating optical tones may cause parasitic optical phase to intensity noise conversion, which may lead to significant increase of mmW phase noise [9]. Although this phase noise impact on the optically generated continuous wave (CW) RF signal induced by the optical paths mismatch has been presented before [10-13], no theoretical investigations on quantification of digitally modulated mmW phase noise degradation by optical self-heterodyning scheme and related impact on the digital signal error vector magnitude (EVM) have ever been carried out.

In this paper, we propose, for the first time to our knowledge, a comprehensive study of phase noise degradation in optical self-heterodyning system and related impact on digital signal EVM. The paper is organized as follows. In section II, theoretical approach for laser phase to intensity noise conversion is presented. In addition, the phase noise induced by the electrical generator employed to generate DSB-SC lightwave has been included in the theoretical model. Furthermore, phase noise measurements of the optically generated mmW signal have been performed and compared with the theoretical results. In section III, broadband mmW up-conversion has been realized by applying high data rate digital signal to the optical self-heterodyning RoF system. Measurement results demonstrate a multi-gigabit per second mmW photonic generation and transmission over 200 m long fiber with the WDM optical self-heterodyning scheme. A theoretical approach to quantify EVM degradation of digital mmW as a function of the optically generated phase noise is performed and compared with measurement results.

Manuscript received June 30, 2011.

Tong Shao (phone: +33456529490, email: shaot@minatec.inpg.fr), Flora Parésys, Ghislaine Maury, Yannis Le Guennec, and Béatrice Cabon are with the Institute of Microelectronics Electromagnetism and Photonics, IMEP-LAHC, Grenoble 38016, France.

Dependence of EVM with optical path difference and laser source coherence time is discussed in the perspective of fulfilling the requirements of 60 GHz ECMA 387 standard [14].

II. Investigation on the Phase Noise Of Optical mmW

Fig. 1 shows the principle of the optical mmW generation based on optical self-heterodyning. In the central station (CS), a Mach-Zhender modulator (MZM #1), which is biased at minimum transmission and driven by a CW signal with the frequency f_{LO} from electrical local oscillator (LO), is employed to generate two optical tones with the interval frequency of $2f_{LO}$. The modulated optical wave is then amplified by the Erbium Doped Fiber Amplifier (EDFA) and sent into the DEMUX, which is employed to select the specific spectral line to each optical channel. Therefore the two optical tones, separated by $2f_{LO}$, are divided in two optical links. One optical tone is modulated with another CW signal at intermediate frequency (IF) f_{IF} from IF generator. The two optical channels are combined and transmitted to the BS for photodetection.

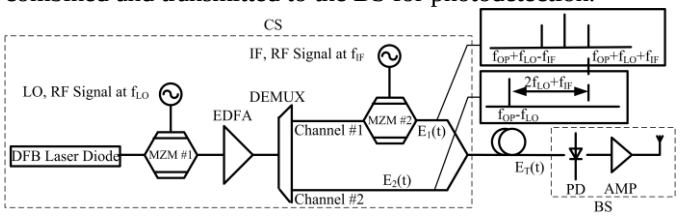

Fig. 1. Principle of the optical self-heterodyning mmW generation

A. Theoretical Analysis of the Photocurrent Phase Noise

We suppose that the optical field of the DFB laser diode is modeled as a quasi-monochromatic amplitude-stabilized field with a phase fluctuation.

The optical field of the laser is expressed as

$$E_{LD}(t) = E_{OP} \exp\left[j\left(2\pi f_{OP} t + \phi_{OP}(t)\right)\right] \tag{1}$$

where E_{OP} is the amplitude of the optical wave, f_{OP} is the central frequency of the optical carrier, $\phi_{OP}(t)$ is the optical phase jitter.

We suppose that the LO and IF generators deliver voltages expressed as

$$\begin{aligned} V_{LO}(t) &= V_{LO}\cos\left(2\pi f_{LO} t + \phi_{LO}(t)\right) \\ V_{IF}(t) &= V_{IF}\cos\left(2\pi f_{IF} t + \phi_{IF}(t)\right) \end{aligned} \tag{2}$$

where V_{LO} and V_{IF} are the voltage amplitude of LO and IF respectively, $\phi_{LO}(t)$ $\phi_{IF}(t)$ are the phase jitter of LO and IF respectively.

When MZM#1 is biased at minimum of transmission, considering (1) and (2), the output optical field of MZM #1 is the DSB-SC light wave, which is expressed as

$$\begin{aligned} E_{MZM\#1}(t) = \frac{\pi}{4} E_{OP} \Big\{ &\exp\left[j\left(2\pi\left(f_{OP} + f_{LO}\right)t + \phi_{OP}(t) + \phi_{LO}(t)\right)\right] \\ &+ \exp\left[j\left(2\pi\left(f_{OP} - f_{LO}\right)t + \phi_{OP}(t) - \phi_{LO}(t)\right)\right]\Big\} \end{aligned} \tag{3}$$

where $E_{MZM\#1}(t)$ is the output optical field of MZM #1 (Fig.1). The output lightwave of MZM #1 contains two spectral lines with the frequency interval of $2f_{LO}$, which are selected by different WDM channels using the DEMUX (Fig. 1). In the BS, the received optical field contains four spectral lines at the frequency of $f_{OP} - f_{LO}$, $f_{OP} + f_{LO}$, $f_{OP} + f_{LO} + f_{IF}$ and $f_{OP} + f_{LO} - f_{IF}$. There is a time delay τ_d, which corresponds to the optical path difference ΔL between channels #1 and #2 before recombination, where $\Delta L = c\tau_d / n$ (c is light velocity in vacuum, n is the refractive index of the optical fiber). Here we only consider the beating of the two spectral lines at frequencies $f_{OP} - f_{LO}$ and $f_{OP} + f_{LO} + f_{IF}$ for the mmW generation. The two optical tones are expressed as

$$\begin{aligned} E_1(t) &= E_1 \exp\Big[j\Big(2\pi\left(f_{OP} + f_{LO} + f_{IF}\right)\left(t+\tau_d\right) + \\ &\phi_{OP}\left(t+\tau_d\right) + \phi_{LO}\left(t+\tau_d\right) + \phi_{IF}\left(t+\tau_d\right)\Big)\Big] \\ E_2(t) &= E_2 \exp\Big[j\Big(2\pi\left(f_{OP} - f_{LO}\right)t + \phi_{OP}(t) - \phi_{LO}(t)\Big)\Big] \end{aligned} \tag{4}$$

where ϕ_{LO} and ϕ_{IF} are the phase jitter of the CW signals at f_{LO} and f_{IF} respectively, E_1 and E_2 are the amplitudes of the two optical spectral lines respectively. Since the coherence time of the electrical generator is much longer than the DFB laser, the impact of delay τ_d on the RF signals could be ignored ($\phi_{LO}(t+\tau_d) = \phi_{LO}(t)$, $\phi_{IF}(t+\tau_d) = \phi_{IF}(t)$).

The photocurrent at the PD output can be calculated as

$$\begin{aligned} &I(t) = E_T(t) E_T^*(t) \\ &= 2E_1E_2 + 2E_1E_2\cos\left(2\pi\left(2f_{LO} + f_{IF}\right)t + 2\pi\left(f_{LO} + f_{IF} + f_{OP}\right)\tau_d + \phi(t)\right) \end{aligned}$$

with

$$\phi(t) = \Delta\phi_{OP}(t, \tau_d) + \phi_{RF}(t)$$

where

$$\begin{aligned} &\Delta\phi_{OP}(t, \tau_d) = \phi_{OP}\left(t+\tau_d\right) - \phi_{OP}(t) \\ &\phi_{RF}(t) = \phi_{IF}\left(t+\tau_d\right) + \phi_{LO}\left(t+\tau_d\right) + \phi_{LO}(t) \approx 2\phi_{LO}(t) + \phi_{IF}(t) \end{aligned} \tag{5}$$

where $\phi(t)$ is the total phase jitter of the photocurrent, which includes the electrical phase jitter induced by the two electrical generators and $\Delta\phi_{OP}(t,\tau)$ which represents the random optical phase change between t and $t+\tau$. $2\pi(f_{OP}+f_{LO}+f_{IF})\tau_d$ represents a constant phase shift, which can be discarded.

The autocorrelation function of the photo current ($R_I(\tau)$) in (5) is expressed as

$$\begin{aligned} &R_I(\tau) = \left\langle I(t) I^*(t+\tau)\right\rangle = \left(E_1E_2\right)^2\left(4 + CC + CC^*\right) \\ &CC = \exp\left(j2\pi\left(2f_{LO} + f_{IF}\right)\tau\right) \times \left\langle \exp j\Delta\phi(t,\tau)\right\rangle \\ &\Delta\phi(t,\tau) = \phi(t+\tau) - \phi(t) \end{aligned} \tag{6}$$

where $\Delta\phi(t,\tau)$ represents the random phase change between t and $t+\tau$. $\langle\rangle$ in (6) presents the mean value over infinite time.

$$\left\langle f(x)\right\rangle = \lim_{T\to\infty}\frac{1}{T}\int_{-\infty}^{+\infty} f(x)\,dx \tag{7}$$

Since the phase jitter of the photocurrent includes the optical phase noise and electrical phase noise, which are totally uncorrelated, $\langle\exp(j\Delta\phi(t,\tau))\rangle$ in the CC term of the photocurrent autocorrelation function (6) can be developed as

$$\begin{aligned} &\left\langle \exp j\left(\Delta\phi(t,\tau)\right)\right\rangle = \left\langle \exp j\left(2\Delta\phi_{LO}(t,\tau)\right)\right\rangle \times \\ &\left\langle \exp j\left(\Delta\phi_{IF}(t,\tau)\right)\right\rangle \times \left\langle \exp j\left(\Delta\phi_{OP}\left(t+\tau,\tau_d\right) - \Delta\phi_{OP}(t,\tau_d)\right)\right\rangle \end{aligned}$$

where

$$\Delta\phi_{LO}(t,\tau)=\phi_{LO}(t+\tau)-\phi_{LO}(t)$$
$$\Delta\phi_{IF}(t,\tau)=\phi_{IF}(t+\tau)-\phi_{IF}(t) \quad (8)$$

$\Delta\phi_{OP}(t,\tau_d)$, $\Delta\phi_{LO}(t,\tau)$ and $\Delta\phi_{IF}(t,\tau)$ are usually assumed to be a zero-mean stationary Gaussian random process respectively [15], the probability density function $W(\Delta\phi(t,\tau))$ of which is defined as

$$\Delta\phi(\tau)=\Delta\phi(t,\tau)=\phi(t+\tau)-\phi(t)$$
$$W(\Delta\phi(\tau))=\frac{1}{\sqrt{2\pi\sigma_{\Delta\varphi}^2(\tau)}}\exp\left[-\frac{\Delta\phi^2(\tau)}{2\sigma_{\Delta\varphi}^2(\tau)}\right] \quad (9)$$

Since $\Delta\phi(t,\tau)$ follows Gaussian distribution, there is the well known relation existed.

$$\left\langle\exp\left[\pm j\Delta\phi(t,\tau)\right]\right\rangle=\exp\left[-\frac{1}{2}\sigma_{\Delta\phi}^2(\tau)\right] \quad (10)$$

Using (10), the autocorrelation function of the photocurrent can be developed as

$$R_I(\tau)=E_0^4\left\{4+2\cos\left(2\pi(2f_{LO}+f_{IF})\tau\right)\exp\left[-\frac{1}{2}\sigma_{\Delta\phi}^2(\tau)\right]\right\} \quad (11)$$

where $\sigma_{\Delta\phi}^2(\tau)$ is the variance of the random optical mmW phase change between t and $t+\tau$. Since the random optical mmW phase change between t and $t+\tau$ contains optical phase change contribution and RF signal phase change contribution, the variance of $\Delta\phi(t,\tau)$ can be developed as [15]

$$\sigma_{\Delta\phi}^2(\tau)=4\sigma_{\Delta\phi_{LO}}^2(\tau)+\sigma_{\Delta\phi_{IF}}^2(\tau)+$$
$$2\sigma_{\Delta\varphi_{OP}}^2(\tau_d)+2\sigma_{\Delta\varphi_{OP}}^2(\tau)-\sigma_{\Delta\varphi_{OP}}^2(\tau-\tau_d)-\sigma_{\Delta\varphi_{OP}}^2(\tau+\tau_d) \quad (12)$$

Hence, the autocorrelation function of the photocurrent is

$$R_I(\tau)=E_1^2E_2^2\left\{4+2\cos\left(2\pi(2f_{LO}+f_{IF})\tau\right)\exp\left[-2\sigma_{\Delta\varphi_{LO}}^2(\tau)-\frac{1}{2}\sigma_{\Delta\varphi_{IF}}^2(\tau)\right]\right.$$
$$\left.\times\exp\left[-\sigma_{\Delta\varphi_{OP}}^2(\tau_d)-\sigma_{\Delta\varphi_{OP}}^2(\tau)+\frac{\sigma_{\Delta\varphi_{OP}}^2(\tau-\tau_d)}{2}+\frac{\sigma_{\Delta\varphi_{OP}}^2(\tau+\tau_d)}{2}\right]\right\} \quad (13)$$

Similarly, the autocorrelation function of the LO ($R_{LO}(\tau)$) and of IF ($R_{IF}(\tau)$) signals can be developed from formula (2) as

$$R_{LO}(\tau)=V_{LO}^2\cos(2\pi f_{LO}\tau)\exp\left[-\frac{1}{2}\sigma_{\Delta\varphi_{LO}}^2(\tau)\right]$$
$$R_{IF}(\tau)=V_{IF}^2\cos(2\pi f_{IF}\tau)\exp\left[-\frac{1}{2}\sigma_{\Delta\varphi_{IF}}^2(\tau)\right] \quad (14)$$

The variance of the random phase change between t and $t+\tau$ ($\sigma_{\Delta\phi}^2(\tau)$) is related to the power spectral density (PSD) of the instantaneous angular frequency fluctuation $S_f(\omega)$ [16]

$$\sigma_{\Delta\phi}^2(\tau)=\frac{\tau^2}{2\pi}\int_{-\infty}^{+\infty}\left[\frac{\sin\frac{\omega\tau}{2}}{\frac{\omega\tau}{2}}\right]^2S_f(\omega)\,d\omega \quad (15)$$

Generally, the random phase change between t and $t+\tau$ ($\Delta\phi(\tau)$) is due to white frequency noise and 1/f frequency noise [17]. The PSD of the signal is found by Fourier transform the autocorrelation function. Therefore, the resulting PSD is the convolution of the PSD due to the white frequency noise and PSD associated with the 1/f frequency noise [17]. We simply ignored the *1/f* noise contribution in the theoretical analysis before investigating its impact in the experimental analysis (section II.B). The instantaneous frequency fluctuation here is considered as white noise for both laser source and electrical generators, which means the PSD of the frequency fluctuation is a constant ($S_f(\omega)=C$), the variance of the random phase change between τ delay ($\sigma_{\Delta\phi}^2(\tau)$) is represented as

$$\sigma_{\Delta\varphi}^2(\tau)=2\gamma|\tau|$$
$$2\gamma=\frac{1}{\tau_c} \quad (16)$$

where 2γ is the angular full linewidth at half maximum (FWHM) of the signal (laser source or pure RF signal) spectrum, τ_c is the coherence time of the source.

By inserting (16) into (13) and (14), the autocorrelation functions of the photocurrent, of the LO and of the IF generator signals are expressed as

$$R_I(\tau)=\begin{cases}E_1^2E_2^2\left[4+2\exp\left(-2\gamma_{OP}|\tau|-(4\gamma_{LO}+\gamma_{IF})|\tau|\right)\right.\\ \left.\times\cos 2\pi(2f_{LO}+f_{IF})\tau\right] & |\tau|\le|\tau_d|\\ E_1^2E_2^2\left[4+2\exp\left(-2\gamma_{OP}|\tau_d|-(4\gamma_{LO}+\gamma_{IF})|\tau|\right)\right.\\ \left.\times\cos 2\pi(2f_{LO}+f_{IF})\tau\right] & |\tau|>|\tau_d|\end{cases}$$
$$R_{LO}(\tau)=V_{LO}^2\cos(2\pi f_{LO}\tau)\exp[-\gamma_{LO}\tau] \quad (17)$$
$$R_{IF}(\tau)=V_{IF}^2\cos(2\pi f_{IF}\tau)\exp[-\gamma_{IF}\tau]$$

where γ_{OP} γ_{LO} γ_{IF} are the angular full linewidth of the laser source and RF signal at f_{LO} and f_{IF} respectively.

The PSD of the photocurrent ($S_I(\omega)$) and of the RF signals at f_{LO} and f_{IF} ($S_{LO}(\omega)$ and $S_{IF}(\omega)$ respectively) are calculated by the Fourier transform of (17).

$$S_I(\omega)=4E_1^2E_2^2\delta(2\pi f)+E_1^2E_2^2\left\{\exp\left(-2\gamma_{OP}|\tau_d|\right)\delta\left(\frac{2\pi(f-f_{mmW})}{2\gamma_{OP}}\right)+\right.$$
$$\left[\exp\left(2\gamma_{OP}|\tau_d|\right)-\frac{\sin\left(2\pi(f-f_{mmW})\right)|\tau_d|}{\frac{2\pi(f-f_{mmW})}{2\gamma_{OP}}}-\cos\left(2\pi(f-f_{mmW})|\tau_d|\right)\right]$$
$$\left.\times\frac{\exp\left(2\gamma_{OP}|\tau_d|\right)}{\pi\left[1+\left(\frac{2\pi(f-f_{mmW})}{2\gamma_{OP}}\right)^2\right]}\right\}*\frac{4\gamma_{LO}+\gamma_{IF}}{(4\gamma_{LO}+\gamma_{IF})^2+(2\pi f)^2}$$
$$S_{LO}(\omega)=V_{LO}^2\frac{\gamma_{LO}}{\gamma_{LO}^2+\left(2\pi(f-f_{LO})\right)^2}$$
$$S_{IF}(\omega)=V_{IF}^2\frac{\gamma_{IF}}{\gamma_{IF}^2+\left(2\pi(f-f_{IF})\right)^2} \quad (18)$$

where $f_{mmW}=2f_{LO}+f_{IF}$, * in (18) indicates the convolution. The PSD of the photocurrent has two components, the optical phase noise contribution and the electrical phase noise contribution.

If we consider a digital modulation on the optically generated mmW, the complex envelope of the broadband photodetected mmW would be expressed as

$$\tilde{x}_{mmW}(t) = \tilde{x}(t)\exp\left(j\phi(t)\right) \tag{19}$$

where $x\square(t)$ is the complex envelop of the ideal broadband digital signal, $\phi(t)$ is the phase jitter of the photocurrent in (5), which is zero-mean Gaussian random process. The phase jitter contains two contributions, which are the phase noise $\triangle\phi_{OP}(\tau_d)$ induced by optical self-heterodyning and the phase noise $\phi_{RF}(t)$ from two electrical generators according to (5). Since the optical phase jitter and electrical phase jitters are totally independent, the variance of the phase jitter can be expressed as

$$\begin{aligned}\sigma_\phi^2 &= \sigma_{\Delta\phi_{OP}}^2 + \sigma_{\phi_{RF}}^2 = \sigma_{\Delta\phi_{OP}}^2 + 4\sigma_{\phi_{LO}}^2 + \sigma_{\phi_{IF}}^2 \\ &= 2\gamma_{OP}|\tau_d| + \left(4\sigma_{\phi_{LO}}^2 + \sigma_{\phi_{IF}}^2\right) = \frac{|\tau_d|}{\tau_c} + \left(4\sigma_{\phi_{LO}}^2 + \sigma_{\phi_{IF}}^2\right)\end{aligned} \tag{20}$$

where $\sigma_{\phi LO}^2$ and $\sigma_{\phi IF}^2$ are the variances of the phase jitters for RF signals at f_{LO} and f_{IF} respectively.

When the optical delay τ_d is large compared to the laser coherence time τ_{cOP}, $\sigma_{\phi LO}^2$ and $\sigma_{\phi IF}^2$ in (20) can be ignored. Indeed, the narrowband electrical phase noise contribution (last term in formula (18)) could be ignored because it is convoluted by a large spectrum component from optical phase noise conversion.

In our self-heterodyning test bench, the optical path difference ΔL is 1.08 m (τ_d=0.0054μs) which corresponds typically to the insertion of a pigtailed MZM. The full linewidth of the laser source is 1.5 MHz, while the coherence time of the laser source (τ_{cOP}) is 0.106μs by the definition of coherence time in (16). The up-conversion frequency $2f_{LO}+f_{IF}$ is 58.32 GHz. The PSD of the photocurrent, which is normalized relatively to its maximum value, is plotted in Fig. 2 by using formula (17). Furthermore, the impact of the phase noise to the constellation diagram for a BPSK digital signal is simulated (inset in Fig. 2) by formula (18) and (19). The simulated PSD of the optical mmW and the constellation diagram will be demonstrated by the experiments.

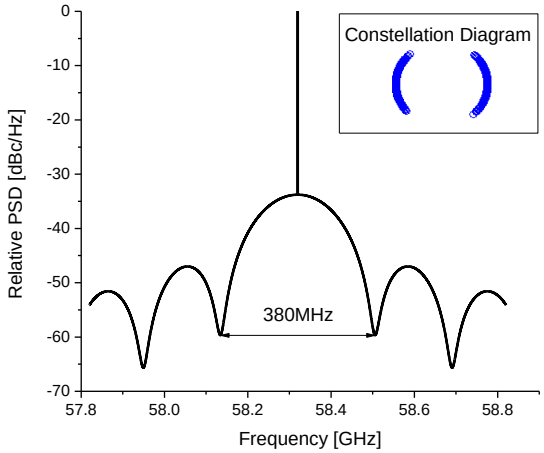

Fig. 2 Simulated power spectral density of the photo current. τ_d/τ_{cOP} = 0.051. Inset: BPSK constellation diagram

When τ_d is small compared to τ_{cOP} ($\tau_d \approx 0$), the PSD of the mmW (discarded the DC component in (17)) will be developed as

$$S_{mmW}(\omega) = \frac{E_1^2 E_2^2}{2\gamma_{OP}} \frac{4\gamma_{LO} + \gamma_{IF}}{\left(4\gamma_{LO} + \gamma_{IF}\right)^2 + \left(2\pi\left(f - 2f_{LO} - f_{IF}\right)\right)^2} \tag{21}$$

Formula (18) and (21) indicate that the PSD of the optical mmW follows Lorentzian slope as the RF signals do, under the assumption of perfect optical paths matching. We need to mention that the result validates only under the assumption that the frequency noise of the optical wave and RF signal only contains white component.

B. Phase noise measurement

The optical mmW is generated by the experimental setup shown in Fig. 1. Limited by the frequency range (40 GHz) of our electrical spectrum analyzer (ESA), we cannot measure mmW at 60 GHz band. During the measurement f_{LO} is set at 25 GHz and f_{IF} is set at 15 GHz. Therefore, the RF signal at $2f_{LO}$ - f_{IF} =35 GHz, which has the same phase noise as the target RF signal at $2f_{LO}$ + f_{IF}, is measured in our experiment. Several optical fibers with different lengths are applied in channel #1 and #2 in order to find the good optical paths matching. The optically generated RF signal spectrums with the large span of 1 GHz for different optical length differences, which take the best path matching as reference, are shown in Fig. 3. Compare Fig. 2 and Fig. 3, the slope of the measured spectrum (Fig.3) agrees with theoretical analysis (Fig.2) in large span, while the optical path difference brings significant phase to intensity noise.

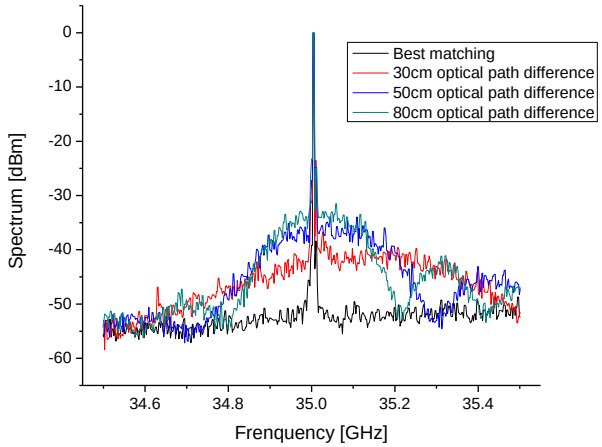

Fig. 3. Spectrum of 35GHz optical mmW with different optical delays

Furthermore, in order to prove that there is no impact of the phase noise due to the optical paths mismatching in our self-heterodyning system, we have measured the single side-band (SSB) phase noise of the optically generated RF signal under the best path matching, compared with the phase noise of the two electrical generators, in Fig. 4. We mention that the phase noise floor is induced by the photodetection of amplified spontaneous emission (ASE) from EDFA (Fig. 1), which is dominant for a frequency offset larger than 1 MHz.

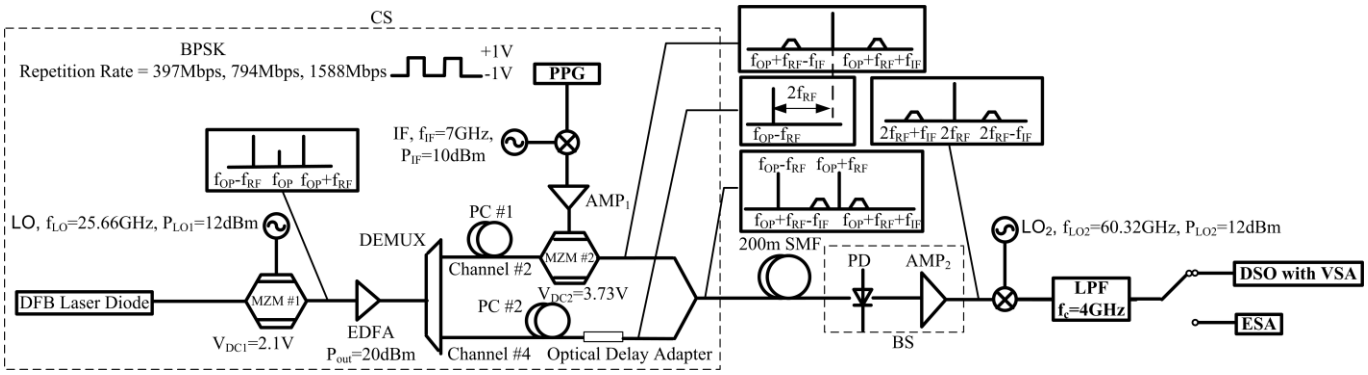

Fig. 5 Experimental setup

CS: Central Station, BS: Base Station, MZM: Mach-Zehnder Modulator, LO: Local oscillator, EDFA: Erbium-Doped Fiber Amplifier, DEMUX: WDM Demultiplexer, PC: Polarization Controller, PPG: Pulse Pattern Generator, AMP: electrical Amplifier, SMF: Single Mode Fiber, PD: Photo Diode, LPF: Low Pass Filter, DSO: Digital Storage Oscilloscope, VSA: Vector Signal Analyzer software, ESA: Electrical Spectrum Analyzer

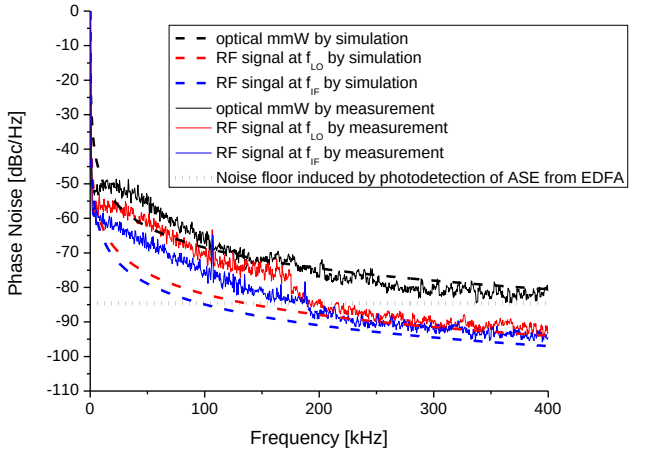

Fig. 4. Measured and simulated single side-band (SSB) phase noises of LO signal (f_{LO}=25GHz), IF signal (f_{IF}=15GHz) and mmW signal ($2f_{LO}$ - f_{IF} =35 GHz) generated with optical self-heterodyning system.

Under the best path matching ($\tau_d \approx 0$), the phase noise PSD of the optical mmW, the RF signals at f_{LO} and f_{IF} from the two electrical generators, which are normalized relatively to the carriers respectively, could be expressed as (22) by using (18) and (21)

$$S_{Inormalized}(f) = 10\log_{10}\frac{(4\gamma_{LO}+\gamma_{IF})^2}{(4\gamma_{LO}+\gamma_{IF})^2+(2\pi(f-2f_{LO}-f_{IF}))^2}$$

$$S_{LOnormalized}(f) = 10\log_{10}\frac{\gamma_{LO}^2}{\gamma_{LO}^2+(2\pi(f-f_{LO}))^2}$$

$$S_{IFnormalized}(f) = 10\log_{10}\frac{\gamma_{IF}^2}{\gamma_{IF}^2+(2\pi(f-f_{IF}))^2} \quad (22)$$

Comparing the measured PSD of RF signal at f_{LO} and f_{IF} in Fig. 4, γ_{IF} is 3 dB lower than γ_{LO}. As a consequence, from the results of the theoretical approach when $\tau_d \approx 0$ (22), the normalized phase noise PSD of the optical mmW is expected 12.2 dB higher than the phase noise PSD of LO generator. Indeed, from Fig. 4, around 400 kHz, we measured that the phase noise PSD of the optical mmW is 12 dB higher than the phase noise PSD of LO generator, which is close enough to the theoretical value found with (22).

Hence the PSD of the optical mmW and RF signal at f_{LO} and f_{IF} by using (22) are shown in Fig. 4 compared to the measurement results. It is obvious that the measured spectrums agree with the theoretical analysis far from the carrier which is the validity domain of the proposed approach considering white frequency noise. From Fig. 4, the measured phase noise PSD for both optical mmW and RF signals close to the carrier are much higher than the theoretical results because of the additional *1/f* noise contributions, which are not taken into account during the theoretical analysis.

Experimental results show that optical path matching can be reached so that optical phase noise to intensity noise conversion does not impact on the optically generated mmW phase noise. When optical path matching is realized, optical mixing process is transparent and mmW phase noise is only impacted by RF source phase noises.

III. High Data Rate mmW Up-Conversion

A. Experimental setup

Self-optical heterodyning system shown on Fig. 1 is now used to generate a high data rate digital signal at 60 GHz band. Fig. 5 shows the configuration of the proposed RoF downlink system. In the CS, a power of 12 dBm CW signal at f_{LO}=*25.66 GHz* is applied to the MZM #1 to generate two spectral lines with the frequency interval of 51.32 GHz. In channel #2 of the DEMUX, The digital signal which drives MZM #2 is a BPSK signal at data rate 397 Mbps, 794 Mbps, or 1588 Mbps corresponding to the values defined by the ECMA 387 standard [14]. It is obtained by mixing of a symmetrical non return to zero (NRZ) base band signal from a pulse pattern generator (PPG) with a CW signal at f_{IF}=*7 GHz*. The BPSK signal is then electrically amplified to reach the power of 10 dBm. As it is said in section II, in order to keep the two optical paths equal, a optical length adapter of 1.08 m optical fiber is applied in channel #4 (Fig. 5). The two optical signals from channel #2 and #4 are combined by using an optical combiner and transmitted through a 200 meter length single mode fiber (SMF) to the BS. This fiber length is typical for the Home Area Network (HAN) applications [18]. As a result of the photo detection in the BS, the PD output signal contains the BPSK modulated signal at

$2f_{LO} + f_{IF} = 58.32$ *GHz*, which is desired, but also a BPSK modulated signal at $2f_{LO} - f_{IF} = 44.32$ *GHz* and a CW signal at $2f_{LO} = 51.32$ *GHz*, which are undesired. Note that the BPSK signal at 44.42 GHz could be removed by using the SSB modulation for MZM #2. The CW signal at 51.32 GHz could be efficiently reused in the up-link system (not investigated in this paper), for frequency down-conversion of the received mmW signal at the BS by an electronic mixer.

Finally, the optically up-converted broadband signal at 58.32GHz band is electronically down-converted and demodulated at 2 GHz band. The broadband signal is mixed with a 60.32 GHz mmW from local oscillator (LO_2) by a mixer with 6 dB conversion loss. The electrically down-converted signal is either digitalized with the Digital Storage Oscilloscope (DSO) and demodulated by the Vector Signal Analyzer (VSA) software (Agilent) or analyzed by using an ESA. A low-pass filter (cut-off frequency f_c=*4 GHz*) is employed before the DSO to filter out all the undesired spectral components. We mention that we do not down-convert the mmW signal to baseband in order to benefit from the synchronization facility provided by the VSA software for coherent demodulation. The Error Vector Magnitude measurement (EVM) is performed by the Vector Signal Analyzer (VSA) software to quantify the quality of the received digital signal.

B. Experimental results

The spectrum and the constellation diagram for 1588 Mbps data rate signal after optical mmW generation and electrical frequency down-conversion are shown in Fig 6. EVM and received power measured after optical mmW generation and electrical frequency down-conversion are reported in Table I, compared with the EVM and emitted power requirements of ECMA 387 standard. We mention that all the results are measured after electrical down-conversion by mixing with another RF signal at 60.32 GHz. EVM values at BS output are in the limit of the ECMA 387 standard to insure error free transmission [1] except for 1588 Mbps data rate. Taken into account the 7 dB down-conversion loss from the mixer, the channel power at 1588 Mbps data rate at BS output can be estimated at around -21 dBm, which is far below the maximum authorized equivalent isotropic radiated power (EIRP) of 10 dBm [1]. Directive antennas could be advantageously used to fit the maximum EIRP.

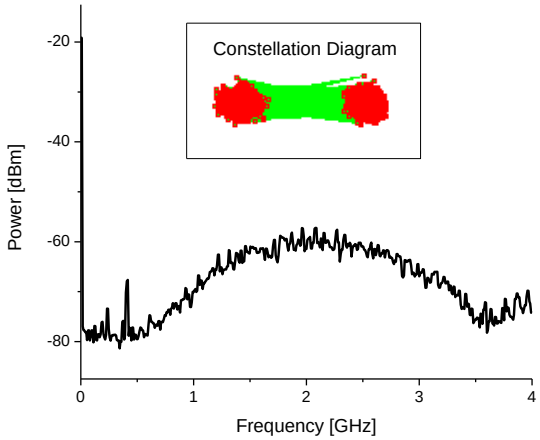

Fig. 6. Measurement results after optical up-conversion of 1588 Mbps BPSK and electrical down-conversion. Inset: BPSK Constellation Diagrams

Table I
Power and EVM measurements without optical phase to intensity noise conversion after electrical down-conversion compared with the requirements of ECMA 387 standard

(i) optical mmW after down-conversion			
Data Rate (Mbps)	397	794	1588
Transmitter Power (dBm)	-20.49	-20.77	-21.44
Power after down-conversion (dBm)	-27.49	-27.77	-28.44
EVM (%)	7.18	9.57	12.56
(ii) ECMA387 requirements for BPSK Signal transmitter and receiver			
Data Rate (Mbps)	397	794	1588
Maximum emitted power (dBm)	10	10	10
Maximum allowed EVM (%)	33.4	23.7	11.2

As it has been discussed in section II and III, the unequal optical paths of the two DEMUX channels can induce phase noise to the broadband signal generated by the self-heterodyne detection. Fig. 6 shows the measured spectrum and constellation (in the inset) after optical self-heterodyning without any optical delay adapter, so that the optical path difference is equivalent to 1.08 m fiber. To see clearly the phase noise impact on the spectrum, the $2f_{LO}$ signal at $2f_{LO}$ =51.32 GHz, which is not modulated by data, is down-converted to 9 GHz. Constellation diagram (inset in Fig. 7) of the electrically downconverted $2f_{LO} + f_{IF}$ exhibits semi-circle. Both spectrum and constellation diagram match very well simulation results shown in Fig. 2. BPSK constellation diagram at 1588 Mbps exhibits thicker semi-circle as in the simulation results (inset Fig. 2) because of the significant impact of the photodetected ASE from EDFA, which has not been taken into account in the theoretical model for simplicity. In the experiment both amplitude noise and phase noise degrade the output signal EVM. EVM measurements for $\tau_d/\tau_{cOP} = 0.051$, which corresponds to 1.08 m different optical fiber length between the two WDM channels (Fig. 5) and 1.5MHz full linewidth of the laser source, are reported in Table. II.

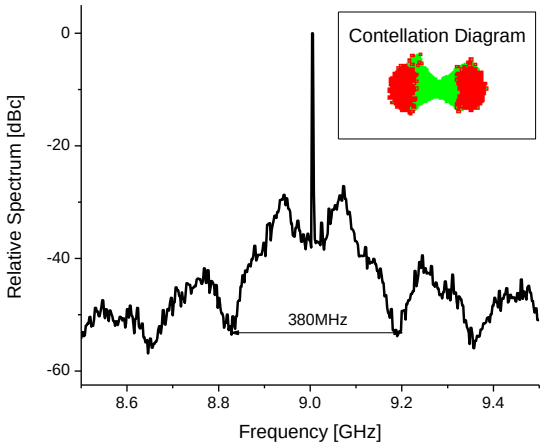

Fig. 7 Measured relative spectrum of the CW optical mmW at 51.32 GHz after electrical down-conversion, τ_d/τ_c=0.051. Inset: constellation diagrams of 58.32 GHz BPSK signal.

Table II
EVM measurements with optical phase to intensity noise conversion after electrical down-conversion $\tau_d/\tau_{cOP} = 0.051$

Data Rate (Mb/s	397	794	1588
EVM (%)	22.3	24.7	27.3

IV. Discussion

Comparing Tables I and II, it is obvious that dominant degradation on the signal quality comes from the impact of the phase noise induced by the optical path difference, hence the importance of the investigation on this point.

EVM is expressed as [14]:

$$EVM = \frac{\sqrt{\frac{1}{N}\sum_{n=1}^{N}\left|S_r(n)-S_t(n)\right|^2}}{R_{\max}} \tag{23}$$

where N is the number of the transmitted symbols, S_r is normalized received symbol, S_t is the ideal transmitted symbol, R_{max} is maximum magnitude of the ideal transmitted symbol for the chosen modulation. The EVM as a function of SNR and σ_φ^2 can be presented as [19]

$$EVM = \sqrt{\frac{1}{SNR}+2-2\exp\left(-\frac{\sigma_\varphi^2}{2}\right)}\sqrt{\frac{1}{PAPR}} \tag{24}$$

where PAPR is the peak to average power ratio for the considered modulation scheme and SNR is the output signal to noise.

We assume that the received symbols contain the phase noise and the amplitude noise, which includes the additive white Gaussian noise (AWGN). The variance of the phase noise has been already investigated in (19). Since additional LO_2 is applied to down-convert the optical mmW, we include a third term which is in the same range of LO phase variance. Therefore the variance of the optical mmW phase jitter is expressed as (20) including the additional phase jitter term from LO_2 for electrical down-convertion:

$$\sigma_\phi^2 = 2\gamma_{OP}\left|\tau_d\right| + \left(4\sigma_{\phi_{LO1}}^2 + \sigma_{\phi_{IF}}^2 + \sigma_{\phi_{LO2}}^2\right) \tag{25}$$

By inserting (25) into (24), the EVM as a function of τ_d/τ_c is expressed as

$$EVM = \sqrt{\frac{1}{SNR}+2-2\exp\left(-\frac{\left|\tau_d\right|}{2\tau_{cOP}}-2\sigma_{\phi_{LO}}^2-\frac{1}{2}\sigma_{\phi_{IF}}^2-\frac{1}{2}\sigma_{\phi_{LO2}}^2\right)}\sqrt{\frac{1}{PAPR}} \tag{26}$$

The CW signals at f_{LO} and f_{IF} are expressed as formula (2). Therefore, the PSD of the CW signals from the electrical generators are generally expressed as [20]:

$$\begin{aligned} S_{LO1}(t) &= \frac{V_{LO1}^2}{2}\delta(f-f_{LO}) + \frac{V_{LO1}^2}{2}S_{\phi_{LO}}(f-f_{LO}) \\ S_{IF}(t) &= \frac{V_{IF}^2}{2}\delta(f-f_{IF}) + \frac{V_{IF}^2}{2}S_{\phi_{IF}}(f-f_{IF}) \end{aligned} \tag{27}$$

And signal powers are derived from (27):

$$\begin{aligned} P_{LO} &= \int_0^\infty S_{LO}(f)df = \frac{V_{LO}^2}{2} + \frac{V_{LO}^2}{2}\sigma_{\phi_{LO}}^2 \\ P_{IF} &= \int_0^\infty S_{IF}(f)df = \frac{V_{IF}^2}{2} + \frac{V_{IF}^2}{2}\sigma_{\phi_{IF}}^2 \end{aligned} \tag{28}$$

The variance of the CW signals of the LO and IF generators ($\sigma_{\phi LO}^2$ and $\sigma_{\phi IF}^2$) can be obtained by integrating the normalized phase noise PSD of the LO and IF generators in Fig. 4.

$$\begin{aligned} \sigma_{\phi_{LO}}^2 &= 2.28\times10^{-4}\,rad^2 \\ \sigma_{\phi_{IF}}^2 &= 7.42\times10^{-5}\,rad^2 \end{aligned} \tag{29}$$

Note that this result is general and takes into account the *1/f* frequency noise found to be dominant in the experimental result under the assumption of perfect optical path matching ($\tau_d=0$) (Fig. 4).

We cannot measure the normalized PSD of the RF signal from LO_2 due to the limited bandwidth of the spectrum analyzer. We assume that the variance of the phase noise for LO_2 used for electrical down-conversion (Fig. 5) is of the same range as the phase variance for LO.

$$\sigma_{\phi_{LO2}}^2 = \sigma_{\phi_{LO}}^2 = 2.28\times10^{-4}\,rad^2 \tag{30}$$

For BPSK modulation scheme, average power is equal to peak power, so that $PAPR=1$. From the EVM values found for the different BPSK data rates when optical path difference is null (Table. I (i)) and from the phase noise variance of the three electrical generators (29) and (30), output SNR of the optical self-heterodyning system can be evaluated for the different BPSK data rates using (26). When the optical path difference is not null, EVM can be evaluated using (26), considering the previously calculated SNR.

In our experiment, the impact of the optical phase to intensity noise conversion induced by 1.08 m different optical fiber length, which corresponds to $\tau_d/\tau_{cOP} = 0.051$(coherence time of the laser source $\tau_{cOP} = 0.106\mu s$), has been measured in section III B (Table. II). Table III shows the calculated output SNR and expected EVM values assuming $\tau_d/\tau_{scOP} = 0.051$ after the aforementioned approach. Comparing Tables II and III, the simulation results are closed to the measurement results.

Table III

SNR and EVM of the BPSK signal by theoretical approach

Data Rate(Mbps)	397	794	1588
SNR (dB)	24.0	21.0	18.4
EVM (%)	23.5	24.4	25.7

Fig. 8 shows the simulation curve of EVM from (26) as a function of τ_d/τ_{cOP} with different SNR from Table III for different data rates in our system. EVM limitations for ECMA 387 standard, for the different data rates, are also reported on Fig. 8.

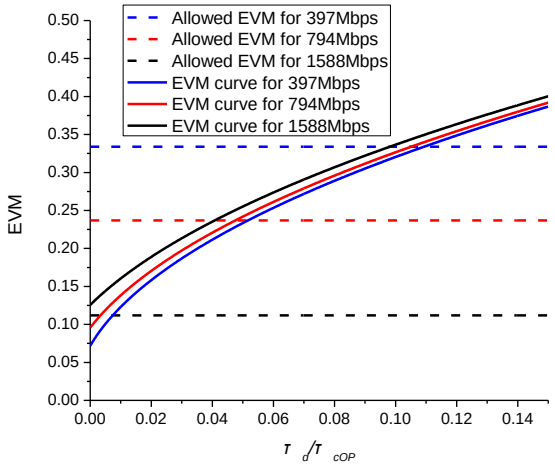

Fig. 8. EVM as a function of τ_d/τ_{cOP} for different data rate optical BPSK signal

According to maximum allowed EVM value given by ECMA 387 standard shown in Table I (ii) and Fig. 8, formula (26) gives the maximum values of τ_d/τ_{cOP} for BPSK signal of different data rate generated by our system, which are shown in Table IV. Since the SNR for the 1588 Mbps signal in our system is already over the limitation to meet the requirement of ECMA 387 standard, there is no way to feed up the EVM requirement by optimizing optical paths matching. Hence, we give the maximum different fiber length, which corresponds to 1.5 MHz full linewidth of the laser source.

Table IV
Max values of τ_D/τ_{COP} for BPSK signal compliant with ECMA 387 standard with laser full linewidth of 1.5 MHz

Data Rate(Mbps)	397	794	1588
Maximum τ_d/τ_{cOP}	0.107	0.046	X
Maximum optical path difference (m)	2.27	0.98	X

As seen in Table IV, for the highest data rate of 1588 Mbps, maximum τ_d/τ_{cOP} cannot be defined because EVM requirements for the ECMA 387 standard is not achieved even with perfect optical path matching (Table. I). Maximum optical path differences found for 397 Mbps and 794 Mbps (Table IV) are in the range of what it can be achieved with commercial pigtailed components. Even if we would use a DFB laser with a higher linewidth of 20 MHz, maximum optical path difference for 397 Mbps and 794 Mbps would decrease but in the range of several centimeters which would be still feasible using commercial components. For the highest data rate of 1588 Mbps, supposing that we manage to improve SNR to fulfill ECMA requirement when $\tau_d = 0$, accurate optical path matching will be more challenging because the margin separating the optimum EVM when $\tau_d = 0$ to the maximum acceptable EVM value will be smaller than for the lower data rates, and also because EVM as a function of τ_d/τ_{cOP} increases fast when τ_d/τ_{cOP} is close to zero (Fig. 8).

V. Conclusion

In this paper, the total phase noise of the optically generated mmW has been theoretically analyzed and experimentally demonstrated by integrating the phase noise contribution of the optical phase to intensity noise conversion, which is induced by a delay in one arm of the self-heterodyning detection, and the RF signals, which are applied to generate the mmW signal. Hence, a good qualified optically up-converted broadband BPSK signal, compliant with ECMA 387 requirements for 387 and 794 Mbps., has been optically up-converted in the 60 GHz band experimentally. Moreover, based on the theoretical investigation on the phase noise, the EVM value as a function of τ_d/τ_{cOP} is deduced and the law of maximum allowed optical path difference is obtained, which would be the key point of WDM DEMUX application on optical mmW generation.

References

[1] N. Guo, R.C. Qiu, S.S. Mo, and K. Takahashi, "60-GHz millimeter-wave radio: Principle, technology, and new results," *Eurasip Journal on Wireless Communications and Networking*, 2007, pp. 8.

[2] Z. Jia, J. Yu, G. Ellinas, and G.K. Chang, "Key enabling technologies for optical-wireless networks: Optical millimeter-wave generation, wavelength reuse, and architecture," *Journal of Lightwave Technology*, vol. 25, no. 11, 2007, pp. 3452-3471.

[3] S. Fukushima, C.F.C. Silva, Y. Muramoto, and A.J. Seeds, "Optoelectronic millimeter-wave synthesis using an optical frequency comb Generator, optically injection locked lasers, and a unitraveling-carrier photodiode," *Lightwave Technology, Journal of*, vol. 21, no. 12, 2003, pp. 3043-3051.

[4] N. Satyan, L. Wei, A. Kewitsch, G. Rakuljic, and A. Yariv, "Coherent Power Combination of Semiconductor Lasers Using Optical Phase-Lock Loops," *Selected Topics in Quantum Electronics, IEEE Journal of*, vol. 15, no. 2, 2009, pp. 240-247.

[5] T. Nakasyotani, H. Toda, T. Kuri, and K.I. Kitayama, "Wavelength-division-multiplexed millimeter-waveband radio-on-fiber system using a supercontinuum light source," *Journal of Lightwave Technology*, vol. 24, no. 1, 2006, pp. 404-410.

[6] M.L. Dennis, J.A. Nanzer, P.T. Callahan, M.C. Gross, T.R. Clark, D. Novak, and R.B. Waterhouse, "Photonic upconversion of 60 GHz IEEE 802.15.3c standard compliant data signals using a dual-wavelength laser," *IEEE Photonics Society, 2010 23rd Annual Meeting of the*, pp. 383-384.

[7] C. Xiangfei, D. Zhichao, and Y. Jianping, "Photonic generation of microwave signal using a dual-wavelength single-longitudinal-mode fiber ring laser," *Microwave Theory and Techniques, IEEE Transactions on*, vol. 54, no. 2, 2006, pp. 804-809.

[8] W. Yong-Yuk, K. Hyun-Seung, S. Yong-Hwan, and H. Sang-Kook, "Full Colorless WDM-Radio Over Fiber Access Network Supporting Simultaneous Transmission of Millimeter-Wave Band and Baseband Gigabit Signals by Sideband Routing," *Lightwave Technology, Journal of*, vol. 28, no. 16, 2010, pp. 2213-2218.

[9] P.T. Shih, C.T. Lin, W.J. Jiang, J. Chen, H.S. Huang, Y.H. Chen, P.C. Peng, and S. Chi, "WDM up-conversion employing frequency quadrupling in optical modulator," *Optics Express*, vol. 17, no. 3, 2009, pp. 1726-1733.

[10] A. Hirata, H. Takahashi, K. Okamoto, and T. Nagatsuma, "Low-phase noise photonic millimeter-wave generator using an AWG integrated with a 3-dB combiner," *Microwave Photonics, 2004. MWP'04. 2004 IEEE International Topical Meeting on*, pp. 209-212.

[11] M.R. Salehi, and B. Cabon, "Theoretical and experimental analysis of influence of phase-to-intensity noise conversion in interferometric systems," *Journal of Lightwave Technology*, vol. 22, no. 6, 2004, pp. 1510-1518.
[12] M.R. Salehi, Y. Le Guennec, and B. Cabon, "Signal and noise conversions in RF-modulated optical links," *Microwave Theory and Techniques, IEEE Transactions on*, vol. 52, no. 4, 2004, pp. 1302-1309.
[13] M. Poulin, C. Latrasse, M. Morin, S. Ayotte, and F. Costin, "Effect of laser decorrelation on the phase noise of RF signals generated by optical mixing of modulation sidebands," *Microwave Photonics (MWP), 2010 IEEE Topical Meeting on*, pp. 253-256.
[14] "http://www.ecma-international.org/publications/standards/Ecma-387.htm. "
[15] P. Gallion, and G. Debarge*Quantum Electronics, IEEE Journal of*, vol. 20, no. 4, 1984, pp. 343-349.
[16] L.S. Cutler, and C.L. Searle, "Some aspects of the theory and measurement of frequency fluctuations in frequency standards," *Proceedings of the IEEE*, vol. 54, no. 2, 1966, pp. 136-154.
[17] L.B. Mercer, "1/f Frequency Noise Effects on Self-Heterodyne Linewidth Measurements," *Journal of Lightwave Technology*, vol. 9, no. 4, 1991, pp. 485-493.
[18] R. Gaudino, D. Cardenas, M. Bellec, B. Charbonnier, N. Evanno, P. Guignard, S. Meyer, A. Pizzinat, I. Mollers, and D. Jager, "Perspective in next-generation home networks: Toward optical solutions?," *Communications Magazine, IEEE*, vol. 48, no. 2, 2010, pp. 39-47.
[19] A. Georgiadis, "Gain, phase imbalance, and phase noise effects on error vector magnitude," *Vehicular Technology, IEEE Transactions on*, vol. 53, no. 2, 2004, pp. 443-449.
[20] F. Hoeksema, R. Schiphorst, and K. Slump, "Spectral Weighting Functions for Single-symbol Phase-noise Specifications in OFDM Systems," *Book Spectral Weighting Functions for Single-symbol Phase-noise Specifications in OFDM Systems*, Series Spectral Weighting Functions for Single-symbol Phase-noise Specifications in OFDM Systems, ed., Editor ed.^eds., 2003, pp.

Tong Shao received M.E degree in optical engineering from Tsinghua University, Beijing, China, in 2009. He is currently working towards Ph.D. degree in Optics and Microwaves at the Grenoble Institute of Technology, Grenoble, France.. His research interests includes study of optical transmission infrastructure, radio over fiber system, and especially optically broadband millimeter wave generation.

Flora Parésys received the degree of the Ecole Normale Supérieure de Cachan, Cachan, France in 2009 and the M. S. from the Grenoble Institute of Technology, Grenoble, France, in 2009. She is currently working toward the PhD degree in Optics and Microwaves at the Grenoble Institute of Technology, Grenoble, France. Her research interests include wireless and optical communication systems especially optoelectronic mixing.

Ghislaine Maury obtained the grade of engineer in telecommunications from Telecom ParisTech in 1995 and the PhD from the Grenoble-INP, Grenoble Institute of Technology in 1998. She is presently assistant professor working in the research group on radio frequency and millimetre waves at IMEP-LAHC laboratory, Institute of Microelectronics, Electromagnetism and Photonics, Grenoble, France. Her research interests include wireless and radio-over-optical fiber systems.

Yannis Le Guennec

Béatrice Cabon (S'93-M'95) is a Professor at Grenoble-INP (Grenoble Institute of Technology France) since 1989. She received the Ph.D. degree in microelectronics from, Grenoble-INP in 1986. From 1986 to 1989, she held a post-doctoral position with the National Center of Telecommunications, Grenoble, France. She was Head (1993-2007) of a research group on RF, Microwaves, Microwave-Photonics techniques at the IMEP-LAHC laboratory in Grenoble, France (Institute for Microelectronics, Electromagnetism and Photonics). She has been coordinator of the club "optics and microwaves" of the French Optical Society (S.F.O) from 1999 to 2008. She has been coordinator of the IST-2001-32786 "NEFERTITI" (Network of Excellence on broadband Fiber Radio Techniques and its Integration Technologies) with 28 organizations over 9 countries, funded by the European Commission (2002-2005). She has been also coordinator of the network of excellence FF6-IST-26592 "ISIS" (InfraStructures for broadband access in wireless/photonics and Integration of Strengths in Europe, www.ist-isis.org, 2006-2009) with 19 organizations of 12 countries. Her research interests include microwave-photonics, photonic-microwave signal processing, optical links for high bit rate signals. She has contributed to over 230 technical publications and is the Editor of four books in these areas.